[10] K. E. Aasmundtveit, E. J. Samuelsen, L. A. A. Pettersson, O. Inganas, T. Johansson, R. Feidenhans'l, *Synth. Met.* **1999**, *101*, 561.
[11] H. Sirringhaus, P. J. Brown, R. H. Friend, M. M. Nielsen, K. Bechgaard, B. M. W. Langeveld-Voss, A. J. H. Spiering, R. A. J. Janssen, E. W. Meijer, P. Herwig, D. M. de Leeuw, *Nature* **1999**, *401*, 685.
[12] a) A. Mechler, J. Kokavecz, P. Heszler, R. Lal, *Phys. Rev. Lett.* **2003**, *82*, 3740. b) N. A. Burnham, O. P. Behrend, F. Oulevey, G. Gremaudi, P. J. Gallo, D. Gourdon, E. Dupas, A. J. Kulik, H. M. Pollock, G. A. D. Briggs, *Nanotechnology* **1997**, *8*, 67.
[13] a) C. Ionescu-Zanetti, K. Cheung, R. Lal, L. P. Lee, *J. Appl. Phys.* **2003**, *93*, 10134. b) F. Houze, R. Meyer, O. Schneegans, L. Boyer, *Appl. Phys. Lett.* **1996**, *69*, 1975.
[14] D. Fichou, F. Charra, A. O. Gusev, *Adv. Mater.* **2001**, *13*, 555.
[15] a) R. Lal, S. A. John, *Am. J. Physiol.* **1994**, *266*, C1. b) C. Ionescu-Zanetti, R. Khurana, J. R. Gillespie, J. S. Petrick, L. C. Trabachino, L. J. Minert, S. A. Carter, A. L. Fink, *Proc. Natl. Acad. Sci. USA* **1999**, *96*, 13175.
[16] H. N. Lin, H. L. Lin, S. S. Wang, L. S. Yu, G. Y. Perng, S. A. Chen, S. H. Chen, *Appl. Phys. Lett.* **2002**, *81*, 2572.
[17] N. F. Mott, R. W. Gurney, *Electronic Processes in Ionic Crystals*, Oxford University Press, London **1948**.
[18] http://www.agfa.com/sfc/pdf/OrgaconPasteTransparant_datasheet.pdf
[19] G. Friedbacher, H. Fuchs, *Pure Appl. Chem.* **1999**, *71*, 1337.

Polyelectrolyte Micropatterning Using a Laminar-Flow Microfluidic Device**

By *Dmitry G. Shchukin*, *Dinesh S. Kommireddy*, *Yongjun Zhao*, *Tianhong Cui*, *Gleb B. Sukhorukov*, and *Yuri M. Lvov**

The study of inter-polyelectrolyte complex formation at interfaces is one of the important areas of interfacial and polymer chemistry. Linear polyelectrolyte,[1] DNA/polyelectrolyte,[2] and protein/polyelectrolyte[3] systems have been studied in bulk solution. Protective, synergetic, catalytic, and hydrophilic (hydrophobic) effects of polyelectrolyte/biomacromolecule combinations could be demonstrated. Such composite polyelectrolyte structures are of practical importance for medical purposes, as components of biosensors, protective coatings, and as biocompatible tools for targeted DNA or enzyme delivery in cells. A number of approaches, including layer-by-layer assembly,[4] mixing of polyelectrolytes in stoichiometric and non-stoichiometric ratios,[1] and in-situ interpolymerization[5] have been developed to provide polyelectrolyte structures with desired composition, properties, and biofunctionality. Ordered, functional polyelectrolyte microstructures allow the production of nanoengineered systems for cell treatment and complex inter-polyelectrolyte sensor elements.[6] Conventional photolithography was used to fabricate such microstructures;[7] however it is not applicable for biological materials, because in photolithographic processes high-energy physical or aggressive chemical treatments are required. Therefore, lithographic methods have strong limitations with respect to the type of materials that can be employed and the resulting microstructures.

One of the most facile and versatile approaches for microfabrication in mild, ambient conditions is laminar-flow synthesis inside microchannels, as proposed by Whitesides and coworkers.[8] This method employs a laminar stream of two or more miscible solutions in one capillary or microchannel. Laminar streams of multiple solutions in the same channel flow individually, and the only method of interaction between dissolved reagents is transverse molecular diffusion. A multiphase laminar-flow approach has been used for the microfabrication of engineered inorganic structures,[8a,b] patterned delivery of cells,[8c] manipulation with lipid bilayers,[9] separation and detection,[10,11] and in the adsorption of protein microstrips.[12] This approach is especially useful in handling proteins, cells, and other delicate biological structures, and it allows control of the spatial delivery of reagents inside microchannels.

In this work, we developed a microfluidic approach for the complex formation of polyelectrolyte and polyelectrolyte/protein microstrips on a glass surface. We also demonstrate experimentally a new, soft micropatterning technique for the anisotropic modification of micrometer-sized objects such as spherical microparticles and polyelectrolyte capsules. Synthesis of poly(dimethyldiallylammonium chloride)/poly(styrene sulfonate) (PDDA/PSS) and poly(dimethyldiallylammonium chloride)/bovine serum albumin (PDDA/BSA) microstrips is demonstrated with a laminar-flow microfluidic reactor. Resulting micropatterns are 8–10 μm wide, separated by a gap of a few micrometers. The width of these microstrips, as well as their position in the microchannel, can be controlled by varying the flow rate and concentration of the individual components.

The synthetic procedure is schematically illustrated in Figure 1. Y- and S-type microchannel reactors (Figs. 1a,b) were employed to realize the formation of inter-polyelectrolyte and polyelectrolyte/protein micropatterns. To fabricate polyelectrolyte microarrays on a glass support, a poly(dimethylsiloxane) (PDMS) membrane with a pattern of channels molded into its surface was placed onto the flat surface of a glass slide (Fig. 1c). Each reactor channel was provided with two inlets and one outlet. Reagents from the inlet channels converge into a single laminar stream in the reactor microchannel. Each reagent solution was gently pumped into its inlet by a KdScientific pump. When two or more liquids flow in parallel at low Reynolds numbers ($Re < 2000$), there is no turbulence

[*] Prof. Y. M. Lvov, Dr. D. G. Shchukin, D. S. Kommireddy, Y. Zhao, Prof. T. Cui
Institute for Micromanufacturing, LaTech
Ruston, LA 71272 (USA)
E-mail: ylvov@coes.latech.edu
Dr. G. B. Sukhorukov
Max Planck Institute of Colloids and Interfaces
1, Am Mühlenberg, D-14424 Potsdam (Germany)

[**] We acknowledge financial support by the National Science Foundation grant NIRT-0210298, Louisiana BoR grant 02/05-RDA19, and from the Sofja Kovalevskaja Program of the Alexander von Humboldt Foundation. We thank A. Khaliq and J. Palmer for help in model computations.

 DOI: 10.1002/adma.200305776

ADVANCED MATERIALS

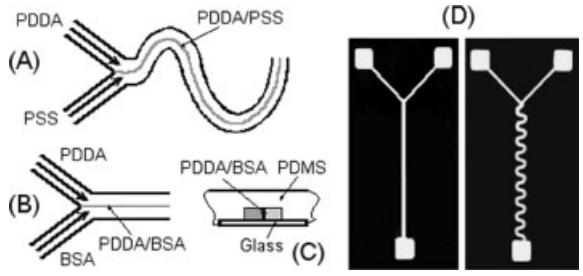

Figure 1. Schematic representation of a laminar-flow patterning experiment. Polyelectrolyte complex formation inside a) S-type microchannels, and b) Y-type microchannels; c) side view, perpendicular to the reactor microchannel; d) microphotographs of channel microreactors.

at the interface between them, and sharp boundaries over the distance of centimeters are maintained. In our device and at the chosen flow conditions, *Re* is about 1 (superlaminar flow). Therefore, the reaction at the interface between the fluid streams is primarily caused by diffusion of the reagents in the transverse direction. Laminar flow controls the spatial delivery of two oppositely charged polyelectrolytes within one microchannel and allows inter polyelectrolyte complex formation with high spatial precision, exclusively at the interface between adjacent streams. The width of the deposited polyelectrolyte microstrip is determined by the diffusion of the reagents across the interface and the flow rates of the solution in the microchannels. Decreasing the diffusion coefficient of the reagents (e.g., by substituting small molecules or solutes (ions) with $D \sim 10^{-5}$ cm^2 s^{-1} with large polyelectrolyte molecules with $D \sim 10^{-7}$ cm^2 s^{-1}) results in the formation of a thin reaction zone of a few micrometers.[13] Delamarche et al.[12] used a similar microfluidic device for protein patterning through adsorption. A typical deposition time was 1 h. In our laminar-flow device, inter-polyelectrolyte complexes formed in 20–30 s, i.e., one hundred times more quickly, and no specific binding of any of the initial reagents onto the bottom of the reactor channel was observed during the entire experiment, which lasted a few minutes.

Introducing solutions of PDDA (1 mg mL^{-1}) and PSS (1 mg mL^{-1}) into the inlet microchannels at the same flow rate (0.01 mL min^{-1}) leads to a reaction at their interface and to inter polyelectrolyte complex formation at the middle of the Y-type reactor microchannel (Fig. 2a). To eliminate stochastic errors, all the synthetic procedures were repeated three times. A similar phenomenon was observed while employing more complicated S-type microchannels. The width of the resulting inter polyelectrolyte pattern mostly depends on the overall concentration of the inlet solutions and ranges from tens of micrometers (for solution concentrations of >2 mg mL^{-1}) to 3–5 μm (for solution concentrations of <0.1 mg mL^{-1}). The ratio between the concentrations of the reagents in the inlet channels did not affect the width of the pattern, and the total flow rate had a minor influence.

Theoretical modeling and analysis for Y-shaped channels were performed to determine the effect of the flow-rate ratio of the inlet channels on the position and width of the PDDA/PSS complex. The interplay of solutions with different flow rates in the two inlets results in a shift of the interface of the interpolyelectrolyte complex towards the side with the lower flow rate (Fig. 2c,d). As the flow rate increases, the volume of the channel occupied by the fluid also increases, causing a latent movement of the diffusion (reaction) zone towards the side with the lower flow rate. An experiment in PDDA/PSS complex formation with different flow rates at the inlets (0.05 mL min^{-1} for the PDDA inlet, 0.01 mL min^{-1} for the PSS

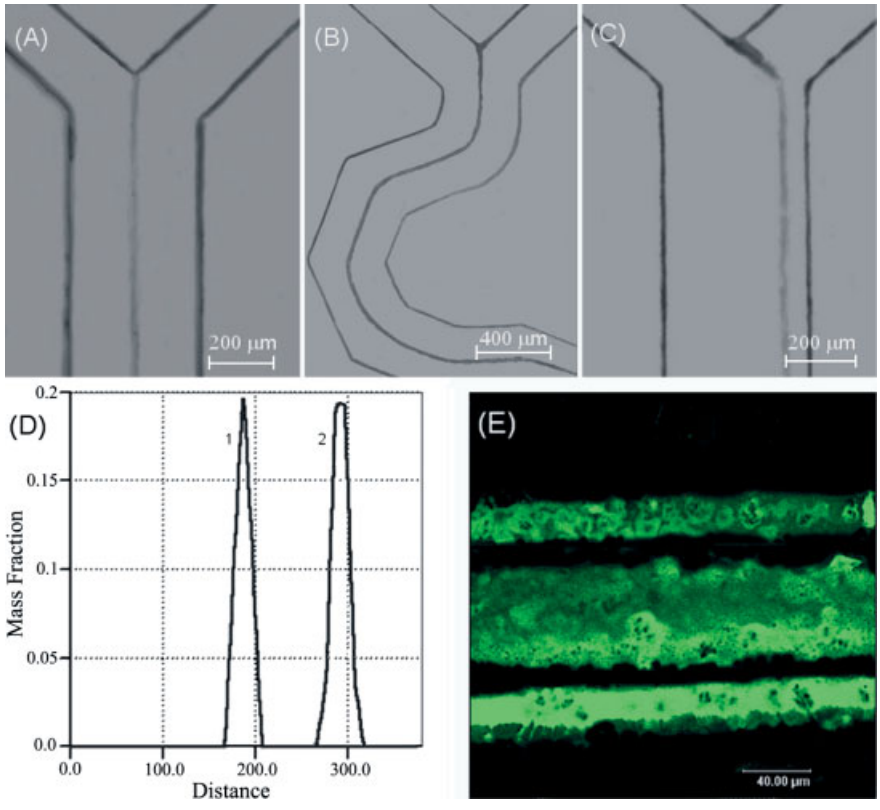

Figure 2. a–c) Optical micrographs of PDDA/PSS microstructures obtained in laminar-flow microreactors. d) Numerical simulation of PDDA/PSS interaction inside a microreactor channel. Mass fraction: quantity of the resulting PDDA/PSS complex. Distance: position of the complex inside a 400 μm channel. Curve 1: microstructure of (a) and (b), flow rates 0.01 mL min^{-1} in both inlets. Curve 2: microstructure of (c), flow rate 0.05 mL min^{-1} (PDDA inlet) and 0.01 mL min^{-1} (PSS inlet). e) Confocal fluorescent image of a PDDA/PSS micropattern on a glass support. PDDA was labeled with FITC. The micropattern was formed by changing the flow rate ratio in-situ from 1:1 (central microstrip) to 1:1.8 and 1.8:1 (lower and upper microstrips).

inlet) confirms the prediction of the simulation (Fig. 2c). Doubling the flow rate in one channel shifts the position of the interpolyelectrolyte complex from the center of the channel by one fourth (ca. 50 μm) in the direction of the low flow rate stream, and vice versa. Therefore, changing the flow rate ratio is an efficient tool for controlling the position of interpolyelectrolyte microstrips.

A flow-rate variation can be performed during the reaction to control the position of interpolyelectrolyte microarrays on the glass support with 5 μm resolution. Fluorescence microscopy visualized the resulting PDDA/PSS micropattern on the glass slide (Fig. 2e), where 20 μm labeled PDDA/PSS strips are separated by 20 μm gaps. A wide central microstrip was obtained at a 1:1 flow ratio and 2 min reaction time. Then, the flow ratio was changed in situ to 1:1.8 and 1.8:1 (lower and upper microstrips, 40 s reaction time for each microstrip). The width and geometry the of interpolyelectrolyte micropatterns are governed by the microchannel geometry, total flow rate (which determines the reaction time), and concentration of the reagents in the inlet channels. By introducing more than two polyelectrolytes into the reactor microchannel (adding more inlet channels), one can form complex inter-polyelectrolyte micropatterns with diverse polymer compositions.

The micrometer-scale resolution observed in the patterns offers the possibility of employing a microfluidic approach for the anisotropic modification of polyelectrolyte microcapsules. The microcapsules could thus be imparted with advanced release and protection abilities. Hollow polyelectrolyte capsules have semipermeable properties and, depending on the pH and ionic strength of the solution, they can release or retain encapsulated material.[14] By modifying part of their wall, unique microcapsules with an anisotropic shell permeability could be fabricated.

To validate the hypothesis that the microfluidic method can be used for selective shell modification, rhodamine-labeled melamine formaldehyde microparticulate templates were adsorbed inside the reactor microchannel prior to introducing a polyelectrolyte solution. Then, in one inlet channel, a fluorescein isothiocyanate (FITC)-labeled dextran solution ($M_w \sim 10\,000$, 1 mg mL^{-1}) was introduced, while the other inlet channel was filled with distilled water. Selective deposition of labeled dextran macromolecules on one half of the template microparticles fixed in the center of the microreactor channel was studied (Fig. 3). Microparticles placed inside laminar streams were either completely covered with dextran or remained unmodified. Therefore, the microfluidic approach allows formation of micropatterns not only on flat substrates but also on the spherical shell of microcapsules, allowing one to change their properties with precise spatial resolution.

BSA was explored as a model protein for studying polyelectrolyte/protein interactions inside a microfluidic reactor. The use of a BSA solution instead of PSS as an inlet reagent (1 mg mL^{-1}) allows formation of a polyelectrolyte/protein pattern deposited directly on the glass support. The thickness of this polyelectrolyte/protein pattern, as illustrated by the fluorescent image in Figure 4, is about 7 μm. The effects of the flow-rate ratio and initial inlet concentrations previously observed for interpolyelectrolyte complex formation were also found for the PDDA/BSA protein complex. The width of the micropattern was adjusted by the initial concentrations of PDDA or BSA, while the position of the micropattern was varied by the flow-rate ratio. Therefore, using laminar flow, it is possible to obtain polyelectrolyte/protein microstrips of predetermined geometry and thickness on a glass support under mild biological conditions.

The structure of the PDDA/BSA complex was studied by atomic force microscopy (AFM, Fig. 4b), which indicated that the PDDA/BSA complex is globular. 300 nm globules and smaller 20–50 nm globules can be identified in the image. Large 300 nm globules were formed during polyelectrolyte/protein complex deposition on glass supports while small 20 nm globules represent initial globular agglomerates of BSA molecules. PDDA/BSA micropatterns on the glass slide can be considered as a PDDA matrix with embedded, separate globular BSA agglomerates.

In conclusion, the laminar-flow microfabrication procedure has been successfully used to produce polyelectrolyte/protein microarrays on the surface of a glass support, and for modify-

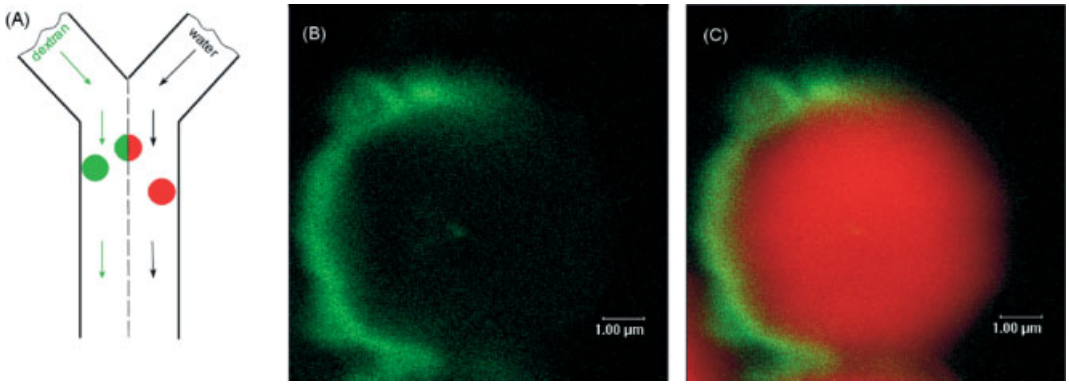

Figure 3. a) Anisotropic micropatterning of rhodamine-labeled microparticulate templates with fluorescein-labeled dextran macromolecules. b) Confocal fluorescent image. c) Overlaid fluorescent image of the resulting anisotropic microparticles.

ADVANCED MATERIALS

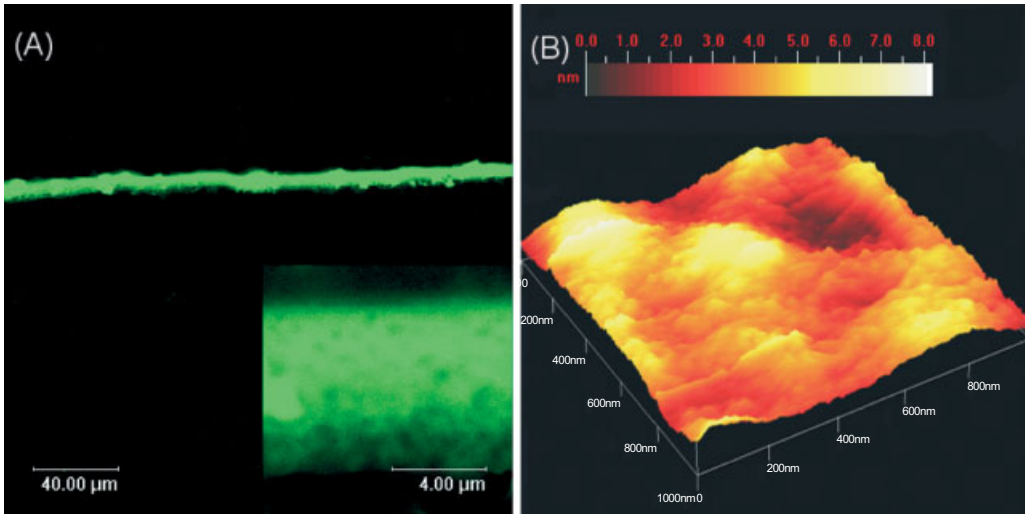

Figure 4. a) Confocal fluorescent image. b) AFM image of a PDDA/BSA microstrip deposited onto a glass support. PDDA was labeled with FITC.

ing microsphere surfaces—both under mild conditions. This simple deposition procedure allows one to obtain 5–10 μm wide strips of proteins complexed with linear polyions on a flat surface. By varying the microchannel structure and flow rate of the reagents, it is possible to fabricate microarrays of different geometry, resolution, thickness, and composition. Selected deposition of labeled dextran macromolecules on one half of the microparticles fixed in the microreactor channel was also elaborated. The resulting micropatterned, bioconjugated structures can be used to produce polyelectrolyte arrays, and they can be utilized as sensor layers, selective bio- (enzymatic) microreactors, and as components of micrometer-scale bioimplants. The application of cells, microcapsules, and blood platelets in assembling micrometer-resolved microarrays and their anisotropic modification by the microfluidic approach are under investigation now.

Experimental

Materials: PDDA (M_W 200 000, Aldrich) and PSS (M_W 70 000, Aldrich) were used to obtain inter-polyelectrolyte micropatterns. For confocal fluorescent spectroscopy, PDDA was labeled with FITC according to the procedure described in the literature [15]. BSA (Sigma) was employed to form polyelectrolyte/protein microstructures. All chemicals were used as received. The water in all experiments was prepared in a three-stage Millipore Milli-Q Plus purification system and had a resistivity higher than 18 MΩ cm. Glass slides, used in all experiments as the support for the polyelectrolyte microstructures, were washed in ethanol and deionized water prior to pattern formation.

Characterization: Confocal microscopy images were obtained with a Leica TCS SP IRE2 (Leica, Germany) scanning system equipped with 10× and 63× oil immersion objectives. Q-Scope 350 Atomic Force Microscope (Quesant Instrument Corporation, USA) operating in tapping mode was used for atomic force microscopy investigations. Microphotographs of complex polyelectrolyte microstructures were acquired with a NIKON Eclipse TS100 (Nikon, Japan) optical microscope.

Simulation: Theoretical modeling for Y-shaped channels was performed with CoventorWare software version 2001.3 (http://coventor.com), a fully integrated microelectromechanical systems (MEMS) design environment, to analyze the effect of solution flow rates on the position of the polyelectrolyte complex in the microchannel. The reaction between PDDA and PSS, PDDA and BSA was assumed to be a first-order, non-reversible, diffusion-controlled reaction. The diffusion coefficient of the polymers in aqueous solutions was taken as 1×10^{-7} cm^2 s^{-1}, and that of BSA was taken as 5×10^{-6} cm^2 s^{-1} [16].

Fabrication of Microchannels: First, lithography on silicon was performed using a thick layer of a positive photoresist. Then, the wafer was etched by inductively coupled plasma etching (Alcatel, 601E, USA) to prepare channels of 200–400 μm. The resulting wafer pattern was used as a mold for the subsequent hot embossing (HEX01/LT, JENOPTIK Mikrotechnik GmbH, Jena, Germany) of a PMMA sheet. This hot-embossing step transfers the channels onto the PMMA sheet as raised lines. A PMMA replica was used as the final mold to form microchannels in a PDMS membrane. To obtain the final PDMS microchannels, PDMS (Sylgard 184 silicone elastomer) and the curing agent (Sylgard 184 curing agent) were mixed in a 10:1 ratio, poured onto the PMMA replica, and heated at 80 °C for 30 min.

Received: July 31, 2003
Final version: December 8, 2003

[1] a) V. Kabanov, *Polym. Sci.* **1994**, *36*, 143. b) F. Brand, H. Dautzenberg, *Langmuir* **1997**, *13*, 2905. c) F. Chaubet, V. Izumrudov, J. Jozefonvicz, *Macromol. Chem. Phys.* **1999**, *200*, 1753. d) B. Philipp, H. Dautzenberg, K.-J. Linow, J. Kotz, W. Dawydoff, *Prog. Polym. Sci., Jpn.* **1989**, *14*, 91.

[2] a) E. Raspaud, M. O. de la Cruz, F. Livolant, *Biophys J.* **1998**, *74*, 381. b) S. Gavryushov, P. Zielenkiewicz, *J. Phys. Chem. B* **1999**, *103*, 5860. c) A. Kabanov, I. Astafyeva, M. Chikindas, *Biopolymers* **1991**, *31*, 1437.

[3] a) V. Izumrudov, *Ber. Bunsenges. Phys. Chem.* **1996**, *100*, 1017. b) E. Seyrek, P. Dubin, C. Tribet, E. Gamble, *Biomacromolecules* **2003**, *4*, 273. c) G. Ladam, C. Gergely, B. Senger, G. Decher, J.-C. Voegel, P. Schaaf, F. Cuisinier, *Biomacromolecules* **2000**, *1*, 674. d) M. Bobreshova, G. Sukhorukov, E. Saburova, L. Elfimova, B. Sukhorukov, L. Shabarchina, *Biophysics* **1999**, *44*, 789. e) J. Gonzalez-Saiz, C. Pizarro, *Eur. Polym. J.* **2001**, *37*, 435.

[4] a) G. Decher, *Science* **1997**, *277*, 1232. b) Y. Lvov, K. Ariga, I. Ichinose, T. Kunitake, *J. Am. Chem. Soc.* **1995**, *117*, 6117. c) P. Hammond, *Curr. Opin. Colloid Interface Sci.* **1999**, *4*, 430. d) H. Mohwald, H. Lichtenfeld, S. Moya, A. Voigt, G.B. Sukhorukov, S. Leporatti, L. Dahne, I. Radtchenko, A. Antipov, C. Gao, *Surfactant Sci. Ser.* **2003**, *109*, 91.

[5] a) M. Antonietti, K. Landfester, *Prog. Polym. Sci., Jpn.* **2002**, *27*, 689. b) M. Antonietti, *Nat. Mater.* **2003**, *2*, 9.

[6] a) Z. Wu, L. Guan, G. Shen, R. Yu, *Analyst (Cambridge, U.K.)* **2002**, *127*, 391. b) S. Park, J. Park, C. Lee, M. Gong, *Sens. Actuators, B* **2002**, *86*, 68. c) A. Diaspro, D. Silvano, S. Krol, O. Cavalleri, A. Gliozzi, *Langmuir* **2002**, *18*, 5047.

[7] a) M. Unger, H.-P. Chou, T. Thorsen, A. Scherer, S. Quake, *Science* **2000**, *288*, 113. b) A. Fu, C. Spence, A. Scherer, F. Arnold, S. Quake, *Nat. Biotechnol.* **1999**, *17*, 1109. c) H. Zheng, I. Lee, M. Rubner, P. Hammond, *Adv. Mater.* **2002**, *14*, 569. d) S. Quake, A. Scherer, *Science* **2000**, *290*, 1536.

[8] a) P. Kenis, R. Ismagilov, G. Whitesides, *Science* **1999**, *285*, 83. b) P. Kenis, R. Ismagilov, S. Takayama, G. Whitesides, S. Li, H. White, *Acc. Chem. Res.* **2000**, *33*, 841. c) S. Takayama, J. McDonald, E. Ostuni, M. N. Liang, P. Kenis, R. Ismagilov, G. Whitesides, *Proc. Natl. Acad. Sci. USA* **1999**, *96*, 5545. d) R. Ferrigno, A. Stroock, T. Clark, M. Mayer, G. Whitesides, *J. Am. Chem. Soc.* **2002**, *124*, 12 930.

[9] L. Kam, S. Boxer, *Langmuir* **2003**, *19*, 1624.

[10] J. Oakey, J. Allely, D. Marr, *Biotechnol. Prog.* **2002**, *18*, 1439.

[11] A. Hatch, A. Kamholz, K. Hawkins, M. Munson, E. Shilling, B. Weigl, P. Yager, *Nat. Biotechnol.* **2001**, *19*, 461.

[12] E. Delamarche, A. Bernard, H. Schmid, A. Bietsch, B. Michel, H. Biebuyck, *J. Am. Chem. Soc.* **1998**, *120*, 500.

[13] S. Takayama, E. Ostuni, P. LeDuc, K. Naruse, D. Ingber, G. Whitesides, *Nature* **2001**, *411*, 1016.

[14] G. Sukhorukov, in *Novel Methods to Study Interfacial Layers* (Eds: D. Möbius, R. Miller), Elsevier, Amsterdam **2001**, pp. 384–415.

[15] G. Ibarz, L. Dahne, E. Donath, H. Möhwald, *Adv. Mater.* **2001**, *14*, 1324.

[16] a) J. Georges, *Spectrochim. Acta, Part A* **2003**, *59*, 519. b) J. Brody, T. Osborn, F. Forster, P. Yager, *Sens. Actuators, A* **1996**, *54*, 704.

High-Conductivity Elastomeric Electronics**

By *Darren S. Gray*, *Joe Tien*, and *Christopher S. Chen**

Flexible electronic circuits have recently gained widespread interest for numerous applications including flexible displays (electronic paper)[1,2] and wearable electronics.[3,4] Despite substantial improvements over rigid devices, current flexible electronics cannot fully conform to their surroundings, due to the inability of metals and conductive polymers to stretch significantly.[5,6] Electronics that could undergo stretching as well as bending would provide additional degrees of freedom in range of motion and prevent damage to both devices and surroundings by matching their mechanical impedances. Currently, to produce a material that is both elastomeric and conductive, metal particles are embedded in an elastomer, such as silicone.[7] This approach is widely used to form interconnections between rigid materials, but the conductivity of such connectors is lower than that of metals and tends to change significantly with strain.[8] Additionally, miniaturization is limited because microfabricated features must be larger than the particle size to ensure conductivity. Here we demonstrate a general strategy to construct elastomeric electronics using microfabricated tortuous wires encased in a silicone elastomer. After a single iteration of geometric optimization, these wires were able to accommodate linear strains of up to 54 % while maintaining stable conductivity. This approach to elastomeric electronics dramatically improves current performance, enabling a range of applications such as forming a direct interface with delicate living tissues or withstanding extreme stress and vibration.

Our strategy for constructing elastomeric electronics is based on the fact that many metals, despite being unable to stretch significantly, are able to bend if their cross sections are sufficiently small. While the common helical spring has been used for centuries to produce a net elongation based on bending, the potential of this simple device to produce stretchable integrated circuits has been largely unexplored. To directly test the hypothesis that integrated circuits made of springs could form the basis of stretchable elastomeric electronics, we used standard lithography techniques[9–11] to embed straight or spring-shaped metal wires in an elastomer (Fig. 1). Circuits, formed by connecting a conductivity meter to exposed contact pads at the ends of the wires, were subjected to linear strain until the point of electrical failure (strain at failure). For ease of microscale manufacture, springs were fabricated in the form of 2D oscillations instead of 3D coils. Gold was the chosen metal, based on its high conductivity, malleability, and chemical inertness.[12] Poly(dimethylsiloxane) (PDMS) was chosen to form the elastomeric "circuit board," mechanically protecting and electrically insulating the wires, based on its durability, adjustable stiffness, biocompatibility, and commercial availability as an insulating compound.[11,13]

When straight wires were strained even minimally (2.4 ± 0.5 %), macroscopic fractures interrupted the flow of current (Fig. 2a, left). Upon allowing the gold wires and their encasing PDMS to return to a strain-free state, the wires regained conductivity, in accordance with the observed return of metal–metal contact at the fracture site. Tortuous wires, containing a wave formed of linked half-ellipses with an amplitude of half the magnitude of the period, remained conductive at a much greater strain of 14.2 ± 0.5 % (Fig. 2a, center). The strain at electronic failure was further improved to

[*] Prof. C. S. Chen, D. S. Gray
Departments of Biomedical Engineering and Oncology
Johns Hopkins University
720 Rutland Avenue, Baltimore, MD 21205 (USA)
E-mail: cchen@bme.jhu.edu
Prof. J. Tien
Department of Biomedical Engineering, Boston University
44 Cummington Street, Boston, MA 02215 (USA)

[**] We gratefully acknowledge funding from the Whitaker Foundation, NIBIB (EB 00262), The Office of Naval Research, and DARPA. We thank Celeste M. Nelson, Srivatsan Raghavan, and John L. Tan for discussions.

DOI: 10.1002/adma.200306107